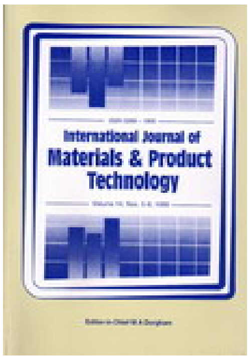

International Journal of Materials and Product Technology

ISSN online: 1741-5209 - ISSN print: 0268-1900
https://www.inderscience.com/ijmpt

Preparation of intelligent responsive printing materials and their application in anti-counterfeiting and packaging

Hong Wu, Xiaorong Zhou, Quan Li

DOI: 10.1504/IJMPT.2026.10078783

Article History:

Received:	09 August 2025
Last revised:	03 December 2025
Accepted:	02 February 2026
Published online:	30 July 2026

Preparation of intelligent responsive printing materials and their application in anti-counterfeiting and packaging

Hong Wu*, Xiaorong Zhou and Quan Li

Department of Art,
Nanchong Vocational and Technical College,
Nanchong 637100, Sichuan, China
Email: wuhong@nczy.edu.cn
Email: zhouxiaorong@nczy.edu.cn
Email: liquan@nczy.edu.cn
*Corresponding author

Abstract: In order to address the challenges of insufficient stability and accuracy in the large-scale application of intelligent responsive printing materials, this paper first designs a dual chamber microcapsule structure with temperature and light dependent response, and applies nano interface crosslinking agents to improve polymer crosslinking density. Secondly, this paper optimises the rheological properties of ultraviolet (UV) ink, adjusts the monomer molecular structure to match surface tension, and makes it suitable for high-speed screen/inkjet printing processes. Finally, this paper constructs a portable detection terminal based on smartphone spectral sensing and support vector machine convolutional neural network (SVM-CNN) algorithm. The results showed that the colour retention rate after five cold chain cycles was 83.33%, the fracture rate after 48 hours of mechanical vibration was only 2.0%, the accuracy of the 5-level high-quality imitation label was 97.5%, and the response threshold drift reached 0.30°C within 96 hours.

Keywords: intelligent responsive printing materials; anti-counterfeiting and packaging; microcapsule structure; environmental tolerance; portable detection.

Reference to this paper should be made as follows: Wu, H., Zhou, X. and Li, Q. (2026) ‘Preparation of intelligent responsive printing materials and their application in anti-counterfeiting and packaging’, *Int. J. Materials and Product Technology*, Vol. 70, No. 6, pp.63–82.

Biographical notes: Hong Wu received her Bachelor degree from Xi’an University of Technology, China. Currently, she works in Nanchong Vocational and Technical College. Her research interests include image processing technology, printing technology and printing materials.

Xiaorong Zhou received her Bachelor’s degree from Beijing Institute of Graphic Communication, China and Master’s degree from China West Normal University. Currently, she works in Nanchong Vocational and Technical College. Her research interests include printing technology, image processing technology, packaging technology and printing materials.

Quan Li received his Bachelor degree from Beijing Institute of Graphic Communication, China. Currently, he works in Nanchong Vocational and Technical College. His research interests include image processing technology, packaging technology and packaging-printing materials.

1 Introduction

As a cutting-edge breakthrough in the field of functional materials, new environmentally responsive printing materials face technical bottlenecks in their large-scale application, a key issue hindering the industry's development. The innovative application of these materials in product anti-counterfeiting and smart packaging is reshaping product safety systems and upgrading user experience (Yang et al., 2025; Shen et al., 2024; Zhou and Miao, 2024). By dynamically sensing external environmental parameters, combined with customised identification features and real-time tracking technology, they effectively achieve enhanced anti-counterfeiting performance and intelligent packaging upgrades (Su and Song, 2021; Singh et al., 2024; Zhu et al., 2025). Against the backdrop of continued advancements in global product safety standards, the development of intelligent material systems that combine multidimensional environmental responsiveness with the advantages of industrial mass production has become a critical research topic in materials science that must be addressed urgently (Yin and Rogers, 2022; Jafarzadeh et al., 2024).

In practical applications, intelligent responsive printed materials face multiple challenges (Ma et al., 2021; Sun et al., 2022). The disconnect between the multidimensional response of anti-counterfeiting characteristics and portable detection technology makes it difficult to popularise efficient, convenient detection methods, hindering the promotion and application of materials and impeding the integration of anti-counterfeiting and packaging. In addition, there is a conflict between the stability of materials in large-scale printing production and their tolerance in complex packaging environments (such as humidity, heat, and mechanical vibration). Although many materials exhibit good response performance under laboratory conditions, they often lack stability in large-scale production (Iftekar et al., 2023). In addition, the materials' insufficient tolerance in packaging environments limits their widespread application in industrial production.

To address these challenges, studies have used various design methods. For example, some studies have improved the response performance and environmental adaptability of materials by modifying polymers and the design of capsule structures (Alidaei-Sharif et al., 2024); some methods have improved the adaptability of materials in the printing process by adjusting the rheological properties of inks (Lopez-Donaire et al., 2023). At the same time, portable detection technology has also been continuously developed. Detection terminals based on smartphone spectral sensing and image recognition algorithms have gradually been applied to the identification of anti-counterfeiting labels (Chen et al., 2022; Han et al., 2024). Although these methods have made progress in some areas, they still face problems such as insufficient integration of multidimensional response characteristics and detection technology, and the contradiction between production stability and packaging adaptability. These problems have not yet been effectively resolved.

To overcome the above bottlenecks, this paper proposes an innovative solution. This study adopts a three-in-one research approach of 'material design, process optimisation, and system integration'. First, we construct a temperature- and light-dual-responsive microcapsule, then regulate the rheological properties of the ultraviolet rays (UV) ink to adapt to high-speed printing, and finally develop a portable recognition terminal based on a smartphone, forming a complete closed loop from material to application. The core lies in the development of a temperature-variable/light-variable dual-chamber microcapsule structure, which, combined with a nano-interface crosslinker, significantly improves the material's wet-heat stability, and by precisely controlling the rheological properties of UV ink, ensures its compatibility with high-speed screen/ink-jet processes. A portable detection terminal based on smartphone spectral sensing and a support vector machine-convolutional neural networks (SVM-CNN) dynamic recognition algorithm is constructed by integrating these technical means. Experimental results show that the solution achieves 97.5% recognition accuracy for high-imitation labels (level 5). The colour retention rate of the material remains 83.33% after five cold chain cycles, and only a 2.0% breakage rate occurred during the 48-hour mechanical vibration test. It effectively solves the key technical barriers in large-scale applications. It paves the way for the practical application of intelligent response materials in the integration of anti-counterfeiting and packaging.

2 Related work

Recent research on intelligent, responsive printed materials has demonstrated significant advances in both material innovation and application expansion. Current research focuses on three dimensions: material design, printing process optimisation, and performance testing, providing valuable insights for this study. At the material design level, Wang et al. (2024a) proposed a composite hydrogel film based on cholesteric liquid crystal microspheres and photochromic spiropyran dyes, which undergo dynamic colour changes in response to temperature and light stimuli, thereby enabling the construction of a multidimensional dynamic anti-counterfeiting label. This research result demonstrates application potential in anti-counterfeiting, security, dynamic camouflage, and bio-inspired driving, but there are still technical bottlenecks in large-scale production and cost control. Muthamma and Sunil (2022) reviewed the applications of cellulose and its nanocellulose derivatives in anti-counterfeiting, explored their potential as environmentally friendly security inks, films, and papers, and analysed the challenges and future research directions for cellulose-based materials in anti-counterfeiting technology.

In contrast, Zhang et al. (2021) began with the latest progress in functional 3D-printing polymer materials and analysed the applications of various functional materials, including electronic conductivity, thermal conductivity, electromagnetic interference shielding, energy storage, and collection. He pointed out the contradiction between material selection and large-scale production, especially the difficulties in functional integration and process adaptation. Although these studies have demonstrated technological potential in various directions, to achieve the accurate commercial application of innovative, responsive materials, core issues such as stability, cost control, and process adaptation for large-scale production remain to be addressed.

In terms of printing process optimisation, controlling relevant properties is crucial for adapting to high-speed printing. Arslan et al. (2023) A studied the flow behaviour and structural recovery properties of inks composed of acrylate-terminated polyurethane-based polyethylene glycol hydrogel precursors and nanoclay Laponite. To ensure efficient printing quality and fluidity, rheological property optimisation is critical. This process can significantly improve the ink's adaptability during printing. Kim et al. (2023) studied the orientation effect of low-concentration bentonite particles in nanocomposites using an embedded 3D printing method and found that this orientation can significantly improve the material's mechanical and physical properties. This study showed that proper particle orientation can enhance the material's stability and structural strength during printing, thereby improving fluidity while optimising printing quality. Soleimani-Gorgani et al. (2021) prepared a water-based UV-curable ink-jet ink in his research and applied it to a transparent flexible polyethylene terephthalate substrate. His research investigated its chemical structure, molecular weight, physical properties, surface tension, and other properties (Soleimani-Gorgani et al., 2021). By rationally adjusting surface tension, adhesion between the ink and the substrate is enhanced, improving the transparency and clarity of the print and guiding improvements in the quality and efficiency of ink-jet printing. Prosvirnina et al. (2022) functionalised the surface of cellulose nanofibres (CNF) produced by bacteria and used them as crosslinking agents and reinforcing agents. They combined them with a polymerisable deep eutectic solvent of acrylic acid and choline chloride to prepare UV-curable ink (Prosvirnina et al., 2022). The study showed that functionalised CNF effectively reduced cellulose agglomeration and improved printing quality. Wang et al. (2024b) designed a unique texture pattern and proposed a triple anti-counterfeiting authentication method that effectively detects product anti-counterfeiting through triple encryption of the texture pattern and three analysis methods, and verified the robustness of the method against various copying methods, devices, and attack scenarios. Although existing studies have provided a variety of ink optimisation strategies, they still face challenges such as stability and cost control in large-scale production.

In research on innovative, responsive printed materials, many scholars have sought to improve their anti-counterfeiting performance and application effectiveness through various technical means. Huo et al. (2022) introduced a method for designing anti-counterfeiting labels using surface-enhanced Raman scattering (SERS) technology and discussed in detail the encoding method of spectral and graphic information in SERS labels. Using these technologies, SERS tags exhibit strong anti-counterfeiting capabilities. However, the development of usable SERS anti-counterfeiting tags for practical applications still faces challenges, including complex production processes and environmental adaptability, and their stability in large-scale production remains to be verified. At the same time, Su H studied the performance of corrugated paper media in cold chain transportation and found that after freeze-thaw treatment, the crystallinity and polymerisation degree of the paper media decreased, the intermolecular hydrogen bonds decreased, and calcium carbonate precipitation and pore size increased on the surface (Su et al., 2023). This research provides valuable experience for improving the stability of cardboard materials in high-humidity environments. However, the durability and damage resistance of these materials in extreme environments still need to be further enhanced to ensure that they can remain effective for a long time during cold chain transportation.

On the other hand, Lin et al. (2024) prepared polymer materials with photochromic, mechanochromic, and thermochromic properties by covalently applying photochromic spiropyran and spirothiopyran (STP) into the polyurethane backbone, and discovered for the first time that white light of a certain intensity can activate STP to produce green. The reversible three-colour change properties of these materials give them strong potential for applications in anti-counterfeiting and information encryption. However, in actual promotion, the durability of the materials and the consistency of their response to external stimuli still need to be overcome. Although existing research has made some progress in innovative anti-counterfeiting materials, many technologies still face challenges in environmental adaptability, complex production processes, and long-term stability.

3 Preparation and process optimisation of smart response materials

3.1 Synthesis of multidimensional dynamic response materials

To realise the application of intelligent responsive materials in anti-counterfeiting and packaging, a dual-chamber microcapsule structure with temperature- and light-dependent responses is designed (Wu et al., 2024; Chen et al., 2025). The left chamber encapsulates a phase-change temperature-sensitive material with sodium oleate as the core, while the right chamber contains photochromic fluorescent dyes (such as spiro pyran derivatives). Through independent response mechanisms, the two chambers achieve decoupled recognition of temperature and light signals, preventing functional crosstalk and ensuring the accuracy and stability of multidimensional dynamic responses. This structure is coated with a composite fluorescent material to achieve the material's multidimensional dynamic response characteristics. In this study, 'multidimensional dynamic response' refers to the composite response ability of materials to temperature changes (thermochromic), ultraviolet light (photochromic), and time-accumulation effects (such as cycle aging), which together constitute the dynamic identification feature space of anti-counterfeiting labels. The specific preparation process is as follows:

Core component of synthetic temperature-responsive materials. Selecting a phase change material (PCM) with a low phase transition temperature, such as sodium oleate, as the core material for the temperature-responsive material and dissolving the PCM in a suitable solvent using solvent evaporation and copolymerising it with the polymer shell to form microcapsules. The thickness of the microcapsule shell is precisely controlled by adjusting the polymer content and reaction time to ensure that the core material stably releases the response signal within the target temperature range. A light-sensitive responsive shell is designed. A fluorescent dye with excellent light-sensitive properties is selected for compounding. A transparent optically variable film is formed by uniformly dispersing fluorescent dyes in an organic polymer matrix through a sol-gel method. This optically variable film exhibits spectral shifts under UV light, which, combined with a temperature-dependent response, enhances the material's multidimensional sensing properties. Dual-responsive materials achieve a synergistic effect by adjusting the hydrophilicity/hydrophobicity of the microcapsule wall. Nanoparticles are dispersed within the microcapsule system as reinforcing agents to improve the material's thermal stability and mechanical strength. In addition, surface functionalisation (e.g., amino and carboxyl groups) is used to enhance the interface compatibility of the microcapsules further, thereby stabilising their dynamic response capabilities across different environmental conditions.

In a hot, humid environment, the addition of a nano-interface crosslinker effectively inhibits microcapsule delamination. The addition of the crosslinker makes the surface interface structure of the microcapsules more compact, improving their tolerance to humidity. Dynamic scanning calorimetry and thermogravimetric analysis (TGA) indicate that the phase transition temperature of the crosslinked microcapsules has increased and that their thermal stability has been significantly enhanced. The synthesised dual-responsive microcapsules are also characterised by X-ray diffraction (XRD), scanning electron microscopy (SEM), and microscopy. SEM images show that the microcapsules have a smooth surface, uniform appearance, and no noticeable cracks, indicating that the integrity and stability of the capsule structure are guaranteed. XRD results show that the composite material has good phase transition properties at low and high temperatures, and its light-sensitive response properties change significantly under ultraviolet irradiation, as shown in Figure 1.

Figure 1 Flowchart of the synthesis of multidimensional responsive materials (see online version for colours)

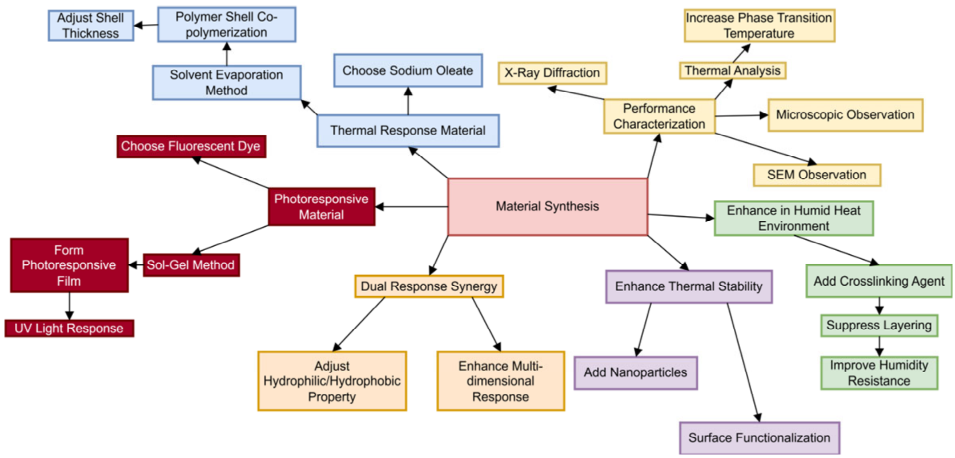

3.2 *Printing adaptability formula optimisation*

To ensure the stable application of innovative responsive materials in high-speed screen printing and ink-jet printing, the rheological properties of UV-curable inks are optimised (Jongprasitkul et al., 2024; Sun et al., 2025) to meet the requirements of different printing processes. The specific optimisation process is as follows:

In the development of UV curing systems, it is necessary to prioritise selecting resin substrates compatible with this process as core components. By regulating the molecular configuration of multiple monomers, precise control of the rheological parameters of the ink can be achieved. Rheological performance testing equipment is used to systematically evaluate the kinematic characteristics of the ink, focusing on ensuring its uniform transmission during the digital printing process and preventing nozzle blockage. On this basis, by optimising the ratio of low-viscosity active monomers to high-viscosity crosslinking components, an ink system with adaptive flow characteristics is constructed, thereby improving printing stability. At the same time, the introduction of specific plasticisers can effectively adjust the intermolecular forces within the ink and improve the system's fluidity.

To adapt to high-speed screen printing processes, the ink's surface tension γ must match the substrate's surface energy. By adjusting the ratio of surfactants and wetting agents in the ink, the surface tension of the ink is altered to ensure even adhesion to different surfaces. By measuring the difference in surface tension between the ink and the substrate, the optimised surface tension matching formula is calculated:

$$\Delta\gamma = \gamma_{ink} - \gamma_{substrate} \quad (1)$$

In formula (1), γ_{ink} is the surface tension of the ink; $\gamma_{substrate}$ is the surface tension of the substrate; and $\Delta\gamma$ represents the surface tension difference between ink and substrate. The smaller the absolute value of $\Delta\gamma$, the better the interface wetting. When $\Delta\gamma$ approaches zero, the ink can spread uniformly on the substrate surface, thereby improving the pattern clarity and adhesion. This parameter is a key indicator for optimising printing suitability.

The optimised ink ensures good adhesion and clear pattern clarity during the screen printing process. To ensure the ink's excellent hardness and durability during UV curing, the photoinitiator content is optimised. By adjusting the photoinitiator ratio, optimising the curing efficiency, and ensuring that the ink cures quickly under UV light, a high-strength cure can be achieved. After UV light exposure, the crosslinking degree of the ink's resin increases, improving the finished product's resistance to scratches, weathering, and water.

3.3 Enhanced dynamic response stability

To improve the stability of innovative, responsive printed materials in hot, humid environments, this study uses a nano-interfacial crosslinker to enhance microcapsule structural stability and inhibit delamination. The nano-interfacial crosslinker is selected and functionalised, enabling it to form a strong chemical bond with the polymer matrix of the microcapsule shell via a chemical crosslinking reaction.

The crosslinked microcapsules are characterised by dynamic thermal analysis and TGA. Thermo-gravimetric analysis can calculate the thermal stability of the material using the following formula:

$$TGA = \frac{Weight\ loss}{Initial\ weight} \times 100\% \tag{2}$$

In formula (2), weight loss is the mass lost by the sample during heating, and initial weight is the initial mass.

To prevent microcapsule delamination due to heat and humidity, a heat-aging test is conducted. The test is conducted under high-temperature, high-humidity conditions to ensure the stability of the microcapsules in such environments. The effect of humidity on microcapsule delamination can be quantified using the following formula:

$$\Delta M = M_{final} - M_{initial} \tag{3}$$

In formula (3), ΔM is the mass change of the microcapsules, and M_{final} and $M_{initial}$ are the mass after hygrothermal aging and the mass of the initial state, respectively. The mass change reflects the degree of moisture absorption and delamination.

To maintain the dual response characteristics of temperature and light changes, crosslinking treatment helps reduce the material's response decay after multiple thermal cycles. The change of phase transition temperature can be evaluated by dynamic scanning thermal analysis, and the phase transition temperature change is calculated using formula (4):

$$\Delta T_{phase} = T_{final} - T_{initial} \tag{4}$$

In formula (4), T_{final} and $T_{initial}$ are the temperatures after and before the phase change, respectively, ensuring that the crosslinked microcapsules can maintain stable dynamic responses under different environmental conditions.

To ensure the material's stability in a complex environment, the surface morphology of the microcapsules is observed using a SEM to verify further the uniformity and stability of the crosslinked microcapsules' surface structure. The surface roughness (R_{MS}) can be calculated using the following formula:

$$R_{MS} = \sqrt{\frac{1}{N}\sum_{i=1}^{N}\left(Z_i - \bar{Z}\right)^2} \tag{5}$$

In formula (5), Z_i is the surface height of the i-th measurement point; $\bar{Z}$ is the average surface height; and N is the total number of measurement points. The surface smoothness of the crosslinked microcapsules is further evaluated through calculation.

To address delamination of microcapsules under hot, humid conditions, it is necessary to systematically quantify the regulatory effect of nanointerfacial crosslinkers on the material's intrinsic stability. Table 1 reveals the structure-activity relationship between crosslink density and structural integrity by using a gradient of crosslinker concentration and designing three key parameter experiments: changes in moisture absorption, phase transition temperature drift, and rupture rate.

Table 1 Relationship between crosslinker addition amount and stability

Crosslinker concentration (wt%)	*Hygroscopic change (%)*	*Phase transition temperature shift (°C)*	*Fracture rate (%)*
0	8.2	–3.5	25.7
1	3.1	–1.2	12.3
1.5	1.5	–0.8	5.4
2	0.9	–0.3	2.1

Notes: The fracture rate refers to the percentage of microcapsules with cracks or fractures in the shell on SEM images after vibration or aging treatment, based on random sampling analysis of at least three fields of view with a total of no less than 500 microcapsules.

Table 1 shows the effect of crosslinker concentration on material stability, including three key parameters: changes in moisture absorption, phase transition temperature drift, and cracking rate. The data show that as crosslinker concentration increases, the change in moisture absorption decreases significantly, indicating that crosslinker application effectively suppresses changes in material quality during moisture absorption. When the crosslinker concentration is 0, the moisture absorption change is 8.2%; at 2 wt%, it drops to 0.9%. In terms of rupture rate, increasing the crosslinker concentration increases material strength, with the rupture rate dropping from 25.7% to 2.1%, demonstrating that the crosslinker significantly enhances the material's tensile strength. Overall, the crosslinking agent increases the crosslink density of the material, thereby enhancing the molecular chain's structural strength, allowing it to exhibit better stability and crack resistance in a humid, hot environment, under temperature changes, and under external forces.

4 Experiment and verification

4.1 Experimental sample preparation

During experimental sample preparation, screen printing and ink-jet printing are used, depending on the application requirements of the anti-counterfeiting label and the smart packaging indicator, respectively. For the screen-printed anti-counterfeiting label, a suitable UV-curable ink is selected, and its rheological properties are adjusted to ensure smooth, stable spraying during the high-precision printing process. During preparation, special attention is paid to controlling the viscosity and curing speed of the ink to ensure clear printing, uniform colour, and good adhesion. In the sample preparation for ink-jet-printed smart packaging indicators, ink fluidity and ink-jet equipment parameters are optimised to meet high-resolution printing requirements. By adjusting the nozzle's jetting frequency, pressure, and other process conditions, the accuracy and consistency of the printed pattern on the paper or plastic substrate are ensured. To ensure the accuracy of the intelligent response function, temperature- and light-variable response materials are selected and embedded in the printing ink to enable dynamic changes in labels and indicators across different environments.

Throughout the sample preparation process, the multidimensional response characteristics of the printed material and the printing process's compatibility are fully considered. Through the gradual optimisation of the printing process, the anti-counterfeiting labels and smart packaging indicators not only achieve the desired anti-counterfeiting effect but also demonstrate excellent stability and dynamic response capabilities in practical applications. Samples are tested under specific environmental conditions to ensure that the prepared samples maintain their functionality and stability at room temperature, in humidity, and under heat.

4.2 Development of portable detection terminals

To enhance the portable detection capabilities of intelligently responsive printed materials, a portable detection terminal based on a smartphone spectral sensor and a dynamic feature recognition algorithm has been developed. The system employs a serial architecture, where a CNN first extracts spatial feature maps from spectral images, then feeds the high-dimensional feature vectors into an SVM for classification. This design balances deep feature extraction capability with robustness in small-sample classification, effectively improving the accuracy of distinguishing highly imitated labels. By integrating spectral sensors and image processing algorithms, this system enables real-time monitoring and identification of temperature- and light-responsive materials. A high-precision spectral sensor covering the visible to near-infrared wavelength range is used to capture high-resolution spectra of material responses. The sensor is connected to a smartphone via its USB port, converting the spectral signal into a digital signal and performing preliminary processing. The spectral data processing model uses the Laplace transform to suppress signal noise, as shown in the following formula:

$$L\{f(t)\} = \int_0^\infty e^{-st} f(t)dt \tag{6}$$

Using a dynamic feature recognition algorithm and machine learning, we analyse the material's real-time temperature- and light-dependent response characteristics. The Laplace transform is mainly used to suppress Gaussian environmental noise (e.g., illumination fluctuations and sensor thermal noise) in the spectrum signal because of its good smoothing properties in the frequency domain. By normalising the collected spectral data, a support vector machine algorithm can be applied to classify and identify different response characteristics. The normalisation formula is as follows:

$$X'' = \frac{X - \mu}{\sigma} \tag{7}$$

In formula (7), X is the original data; μ is the mean; σ is the standard deviation; and X' is the normalised data. The SVM-based classification model can accurately classify the response signal across different environments, effectively distinguishing true and false labels. To enhance detection accuracy, a convolutional neural network is trained to recognise image data by combining spectral features and dynamic response models. After the image is input, the response features are extracted through multiple convolution and pooling layers, and the classification results are finally output. The convolution operation formula of the convolution layer is:

$$y(t) = (x * w)(t) = \int_{-\infty}^{\infty} x(\tau) w(t - \tau) d\tau \tag{8}$$

To ensure the miniaturisation and convenience of the terminal device, the system develops an image-acquisition module for a smartphone. This module uses a built-in camera and a dedicated light source to capture the label and, using a processing algorithm, calculate its colour difference. Under temperature change response, the colour difference formula is used to evaluate the response change:

$$\Delta E_{00} = \sqrt{\left(L^* - L_1\right)^2 + \left(a^* - a_1^*\right)^2 + \left(b^* - b_1^*\right)^2 + R_1 C_1} \tag{9}$$

In formula (9), L^*, a^*, and b^* are the chromaticity, saturation, and brightness components, respectively, and ΔE_{00} is the colour difference, which reflects the visual change of the response. By experimentally verifying the responsive material under different lighting conditions, an adaptive dimming algorithm is developed to optimise the spectral capture accuracy under environmental changes. The following formula can describe the relationship between light intensity and signal capture:

$$I_{signal} = I_{incident} \cdot e^{-\alpha d} \tag{10}$$

In formula (10), I_{signal} is the received signal intensity; $I_{incident}$ is the incident light intensity; α is the material absorption coefficient; and d is the light propagation distance.

4.3 Quantifying the difficulty of imitation of anti-counterfeiting features

To validate solutions to the environmental tolerance bottleneck in large-scale printing, it is necessary to evaluate the impact of high-precision equipment on dynamic response consistency. By establishing a five-level equipment gradient model (level 1 basic to level 5 precision), the correlation between equipment level, operating time, and response deviation is quantified. The results are shown in Figure 2.

Figure 2 Analysis of imitation difficulty and dynamic response consistency, (a) relationship between device level and working hours (b) distribution of device level and response consistency deviation (see online version for colours)

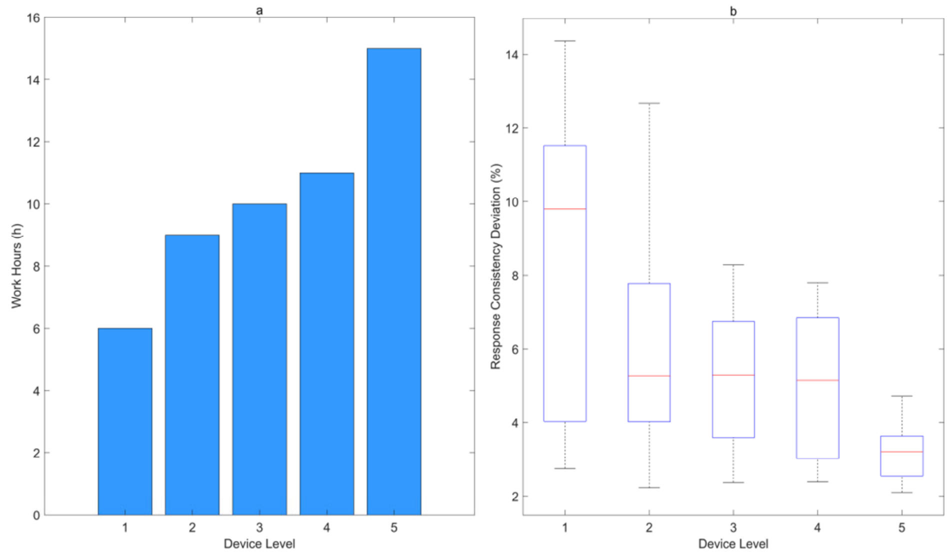

Figure 2 reveals the correlation between device level, work duration, and response consistency deviation. The response consistency deviation is the relative standard deviation of the dynamic response values (e.g., colour difference or spectral peak position) across multiple printed samples under the same equipment and process conditions, relative to their mean. It is used to measure the stability of the response output. The data shows that as the device level increases from level 1 to level 5, work duration increases from 6 hours to 15 hours, while the mean response deviation decreases significantly from 8.8% to 3.2%. Level 1 devices exhibit significant deviation fluctuations, while level 5 devices exhibit a stable, narrowing deviation range of 2.10% to 4.73%. This reversal confirms the core requirement for high-precision printing: equipment stability enables advanced equipment to maintain a consistent response over the long-term. This phenomenon stems from two aspects: the synergistic effect of the temperature-variable/light-variable dual-chamber microcapsule structure and the nano-interface crosslinker, which significantly enhances the material's wet and hot stability, so that the deviation of the level 5 equipment remains stable below 5% during 15 hours of continuous operation, solving the environmental tolerance bottleneck of large-scale printing. The rheological properties of UV ink are optimised to adapt to high-speed screen/ink-jet processes. Combined with real-time calibration of the dynamic recognition algorithm on smartphones, the equipment deviation fluctuation range is compressed from 11.6% at level 1 to 2.62% at level 5, breaking through the technical barriers to dynamic response materials in high-precision printing of anti-counterfeiting labels.

4.4 Dynamic response cycle stability

Given the risk of response degradation under cyclic stress, it is necessary to compare the long-term reliability of the new dual-chamber microcapsules with that of traditional materials. Traditional materials refer to single-chamber temperature-sensitive microcapsule systems without a double-chamber structure and a nano-crosslinking agent, whose shells are composed of ordinary polyurethane with low crosslinking density, which are prone to rupture or response attenuation under hot, humid conditions or mechanical stress. Through temperature-dependent cycling accelerated aging experiments, structural stability (colour difference/cracking rate) and functional durability (response time/detection accuracy) are simultaneously monitored. The results are shown in Figure 3.

Figure 3 Comparative analysis of cyclic stability and system performance of innovative response materials, (a) comparison of material structural stability and functional durability (b) comparison of response efficiency and system performance (see online version for colours)

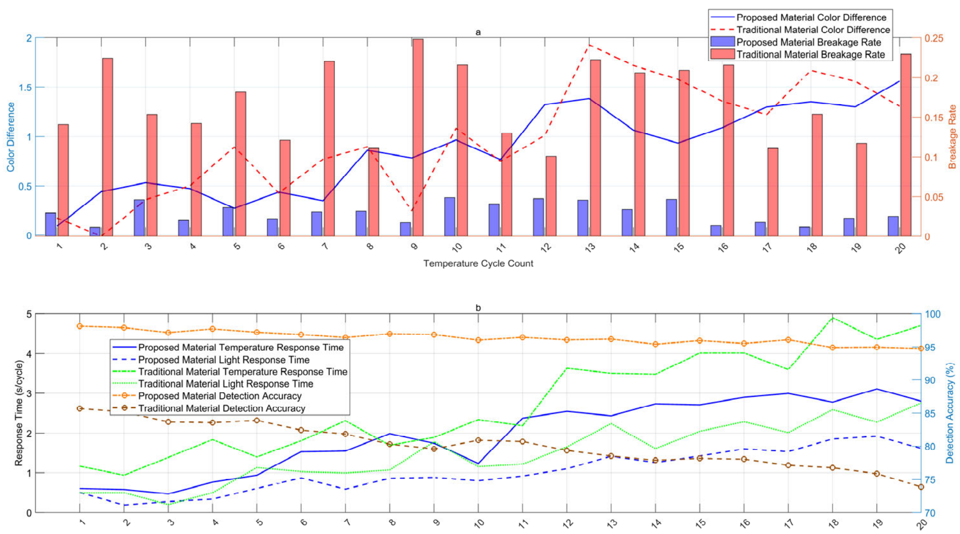

Figure 3(a) compares the structural stability and functional durability of the materials through the number of temperature cycles. The colour difference value of the novel material steadily increases from an initial 0.09 to 1.56, while the traditional material experiences significant fluctuations, reaching a peak near 1.93. The crack rate of the novel material remains stable between 1.1% and 4.9%, while that of the traditional material is as high as 10% to 25%. Figure 3(b) reveals the difference in response efficiency: the temperature-change response time of the new material increases from 0.47 s to 3.10 s, and the light-change response time increases from 0.19 s to 1.92 s, both of which are significantly lower than the traditional material temperature-change response time of 0.94 s to 4.90 s and light-change response time of 0.21 s to 2.76 s. The detection accuracy of the novel material decreases slightly from 98.1% to 94.8%, while that of the traditional material decreases from 85.7% to 73.9%, highlighting the novel material's performance advantage under cyclic pressure. The dual-chamber microcapsule structure isolates the temperature- and light-responsive materials, preventing functional crosstalk. The nano-interface crosslinker reduces the breakage rate of the novel material and maintains structural integrity by increasing the polymer crosslink density.

4.5 Portable detection performance verification

To ensure the adaptability of portable detection systems in complex scenarios, it is necessary to examine how sample complexity affects recognition performance. By constructing a five-level counterfeit labelling model (from level 1, simple, to level 5, high-quality), the correlations among complexity, recognition accuracy, false-positive rate, and time consumption are analysed under unified detection conditions. The results are shown in Figure 4.

Figure 4 Analysis of the impact of sample complexity on the performance of portable detection systems (see online version for colours)

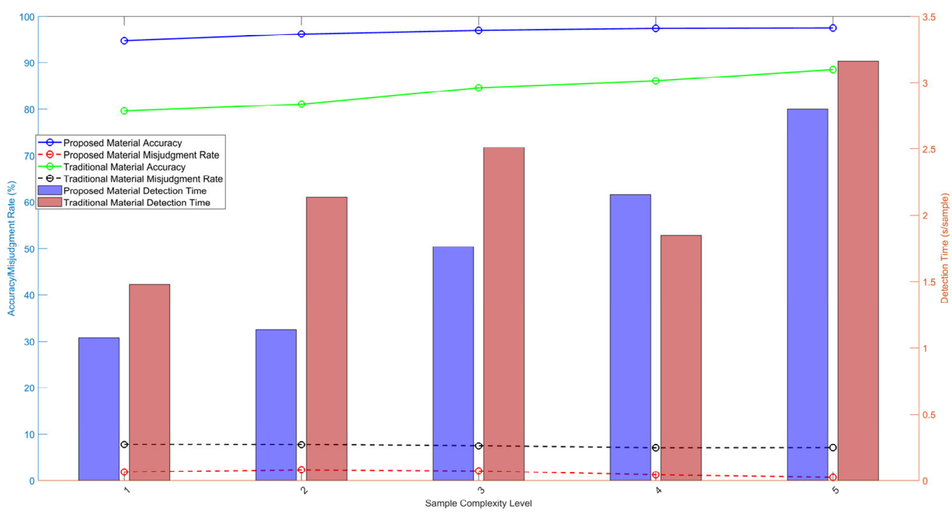

Figure 4 reveals the significant impact of sample complexity (levels 1–5) on the detection system. As complexity increases (from simple level 1 labels to high-fidelity level 5 labels), the recognition accuracy of novel materials steadily increases from 94.7% to 97.5%. The false positive rate decreases from 1.8% to 0.7% for novel materials and from 7.8% to 7.1% for traditional materials. The difference is further highlighted by the test-time data: the new material takes 2.80 seconds at level 5 complexity, while the traditional material takes 2.51 seconds at level 3 and 3.16 seconds at level 5. This performance advantage is due to a dual technological innovation: a SVM-CNN hybrid model is used to eliminate environmental noise through normalisation. The dual-chamber microcapsule structure produces a stable phase-difference signature, which the algorithm accurately extracts using a convolutional kernel, reducing the computational effort required to identify high-quality counterfeit labels. When processing at level 5 complexity and using Laplace transforms for noise suppression, the false positive rate decreases, demonstrating the enhanced anti-counterfeiting detection performance achieved through a collaborative design of material and algorithm. At the same time, to ensure the universality of the portable detection terminal in actual scenarios, its robustness under various environmental conditions must be verified. By setting temperature and humidity gradients, light intensity (50 lux), and dynamic scanning conditions, and using traditional materials as a control group, the impact of environmental variables on dynamic feature recognition accuracy, false positive rate, and detection efficiency is quantified. The results are shown in Table 2.

Table 2 Comparison of environmental adaptability of portable detection terminals

Environmental conditions	*Dynamic feature recognition accuracy (%)*		*Counterfeit label misjudgement rate (%)*		*Detection time (s)*	
	New material	*Traditional material*	*New material*	*Traditional material*	*New material*	*Traditional material*
Room temperature and humidity (25°C, 50%RH)	98.7±0.3	85.2±2.1	1.2±0.4	14.8±3.2	0.8±0.1	2.5±0.6
High temperature and high humidity (40°C, 85%RH)	96.5±0.8	72.3±4.7	3.1±0.9	27.5±5.3	1.2±0.3	3.8±1.1
Low light environment (50 lux)	95.2±1.2	68.7±5.2	4.3±1.1	31.2±6.1	1.5±0.4	4.2±1.3
Fast moving scan	93.8±1.5	60.5±6.8	6.0±1.8	39.7±7.4	0.9±0.2	3.5±0.9

Table 2 shows that at 25°C and 50% relative humidity, the new material's dynamic feature recognition accuracy is 98.7±0.3%, higher than the 85.2±2.1% of the traditional material. The false-positive rate for counterfeit labels is 1.2±0.4%, compared with 14.8±3.2% for the traditional material. The detection time for the new material is 0.8±0.1 seconds. This demonstrates that the new material can maintain high recognition accuracy even in extreme environments such as high temperature, high humidity, and low light. Traditional materials exhibit significant performance fluctuations under environmental stress, leading to higher false-positive rates and longer detection times. The new material also shows high efficiency in fast-motion scanning tests, highlighting its advantages in efficient, high-precision anti-counterfeiting recognition scenarios.

4.6 Packaging service environment tolerance

To meet the application needs of innovative packaging in extreme environments, such as cold chains, it is necessary to evaluate the performance evolution of materials under conditions of damp-heat aging and sudden temperature changes. By simulating accelerated damp-heat aging for 0 to 96 hours and performing dual-stress field tests with 1 to 5 cold-chain cycles, the material's response threshold drift and colour retention rate are monitored. The cold cycle refers to the alternation between –18°C (frozen) and 4°C (refrigerated). Each cycle lasts 12 hours, for a total of five cycles, to simulate the typical temperature fluctuations encountered in cold chain transportation of fresh food and to evaluate the colour stability of materials in practical applications. The results are shown in Figure 5.

Figure 5 Comparison of material environmental tolerance under wet heat aging and cold chain cycle (see online version for colours)

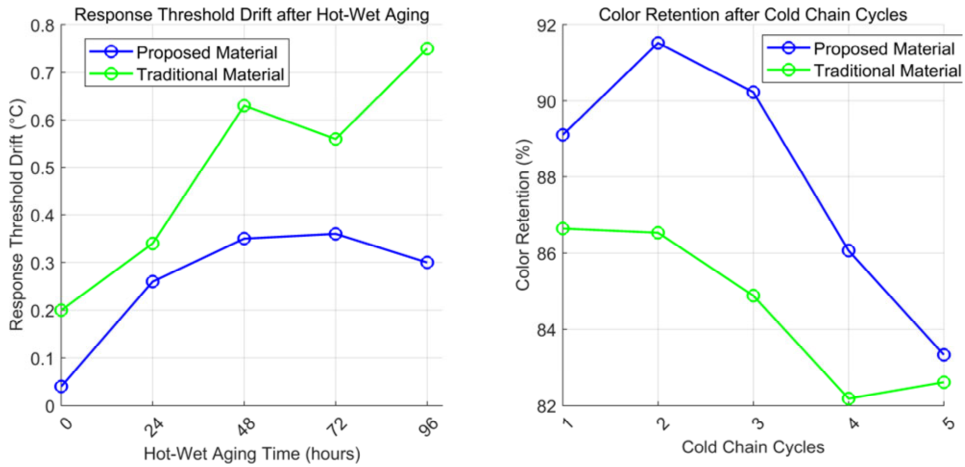

Figure 5 shows the effects of the damp-heat aging time (0–96 hours) and the number of cold chain cycles (1–5) on material performance. During damp-heat aging, the response threshold drift of the new material gradually increases from an initial 0.04°C to 0.30°C, whereas the traditional material increases dramatically from 0.20°C to 0.75°C. In the cold chain cycle data, the colour retention rate of the new material reaches a peak of 91.52% in the second cycle and remains at 83.33% in the fifth cycle; the traditional material drops from 86.64% to 82.61%, and reaches the lowest value of 82.18% in the fourth cycle, indicating that it is not stable enough when the temperature changes suddenly. This difference stems from the crosslinking agent's strengthening effect. The dense network formed by the crosslinking agent on the microcapsule's surface reduces the new material's water absorption rate. It effectively inhibits the expansion and deformation during wet heat aging. The dual-chamber microcapsule structure provides synergistic protection, and the uniform dispersion of the photovariable fluorescent dye within the crosslinked polymer matrix ensures that the colour retention rate during the cold chain cycle is consistently higher than that of traditional materials. During the fifth cold cycle, the new material maintains colour stability through the phase-change temperature compensation mechanism. In contrast, the traditional material suffers from irreversible structural degradation due to phase-change temperature drift.

To verify the effectiveness of intelligent, responsive materials in real cold-chain packaging scenarios, this study designs a food freshness indicator experiment based on temperature- and light-responsive materials. Fresh salmon fillets, a representative of perishable cold chain foods, are selected as the test subject. Indicator labels incorporating the novel innovative response material are affixed to salmon packaging bags. The entire experiment is conducted in a simulated cold chain environment (4°C). Samples are collected at 0 hours (initial), 24 hours, 48 hours, 72 hours, and 96 hours. At each time point, TVB-N content determination and label colour reading were performed simultaneously on the same packaging sample to ensure data consistency. Food spoilage indicators: The total volatile elemental nitrogen (TVB-N) content of salmon is measured using national standard methods as a key chemical indicator for objectively evaluating freshness (TVB-N ≥ 20 mg/100g generally indicates spoilage). The relevant changes are shown in Figure 6.

Figure 6 Relationship between the colour change of the smart response indicator label and the TVB-N value of salmon (see online version for colours)

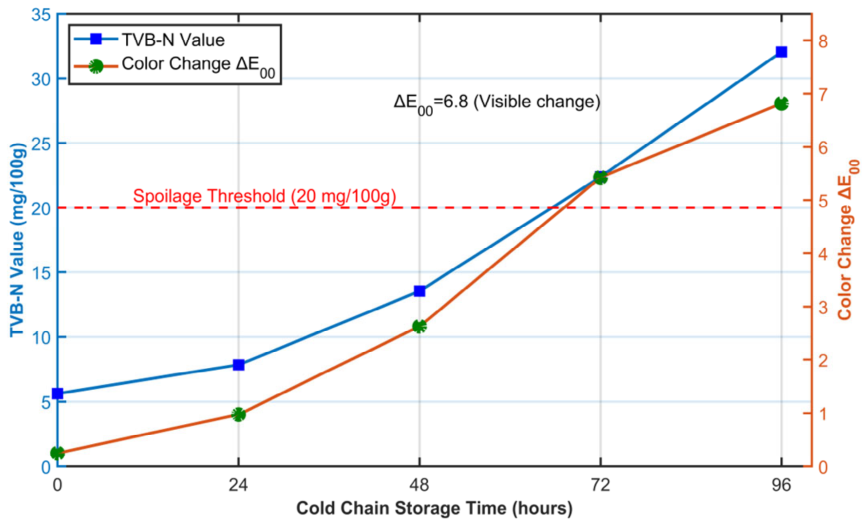

As shown in Figure 6, the TVB-N value of salmon increases with storage time, reaching 32.0 mg/100 g at 96 hours, indicating significant spoilage. At the same time, the colour difference ΔE_{00} of the smart indicator label also shows a regular increase. When the TVB-N value exceeds 32 mg/100 g, the label's ΔE_{00} reaches 6.8, and the colour change is significant enough for consumers to identify as a 'stale' signal intuitively. The current ΔE-TVB-N correlation is based on salmon data, and because of differences in metabolic pathways involved in food spoilage, this mapping lacks universal applicability. However, this smart label can achieve customised freshness indication by calibrating the critical TVB-N thresholds for different foods.

To address the mechanical vibration risks during packaging and transportation, it is necessary to evaluate the failure behaviour of materials under continuous vibration. Using traditional materials as a benchmark, a 12–48-hour step-vibration test is conducted to monitor mechanical tolerance indicators, including failure rate, colour change, and microcapsule rupture rate. The results are shown in Table 3:

Table 3 presents data on the packaging material's tolerance to mechanical vibration, including failure rates, colour variations, and microcapsule rupture rates for the new and traditional materials at different vibration durations. After 12 hours of vibration, the failure rate for the new material is 1.2±0.3%, lower than the 15.3±2.1% for the traditional material. The comparison of colour difference changes and microcapsule rupture rates also shows the advantages of the new material in these two indicators: 0.8±0.2 % and 0.5±0.1%, respectively, compared with 3.5±0.7 % and 8.7±1.3% for traditional materials, indicating that the new material has better stability and tolerance to vibration. The microcapsules and overall structures of traditional materials may not withstand long-term vibration effectively, leading to a higher failure rate and greater colour differences. In addition, as vibration duration increases, the rupture rate of traditional materials rises sharply. In contrast, the new material effectively resists vibration-induced microcapsule damage, demonstrating better vibration tolerance, especially in packaging applications, where it can provide higher reliability and safety.

Table 3 Mechanical vibration tolerance of packaging materials

Vibration duration (h)	*Failure ratio (%)*		*Colour difference*		*Microcapsule rupture rate (%)*	
	New material	*Traditional material*	*New material*	*Traditional material*	*New material*	*Traditional material*
12	1.2±0.3	15.3±2.1	0.8±0.2	3.5±0.7	0.5±0.1	8.7±1.3
24	3.8±0.7	28.6±3.5	1.5±0.3	5.2±1.1	1.2±0.3	15.2±2.4
48	7.5±1.2	42.1±4.8	2.3±0.5	7.8±1.6	2.0±0.5	24.3±3.1

4.7 Printing process compatibility assessment

To adapt to high-speed screen/inkjet printing processes, it is necessary to understand how printing resolution affects material suitability. By setting a DPI gradient (100–500), the changing trends of dot gain (printing accuracy) and ink adhesion (printing durability) in the two processes are measured. The results are shown in Figure 7.

Figure 7 Effect of printing resolution on material printability (see online version for colours)

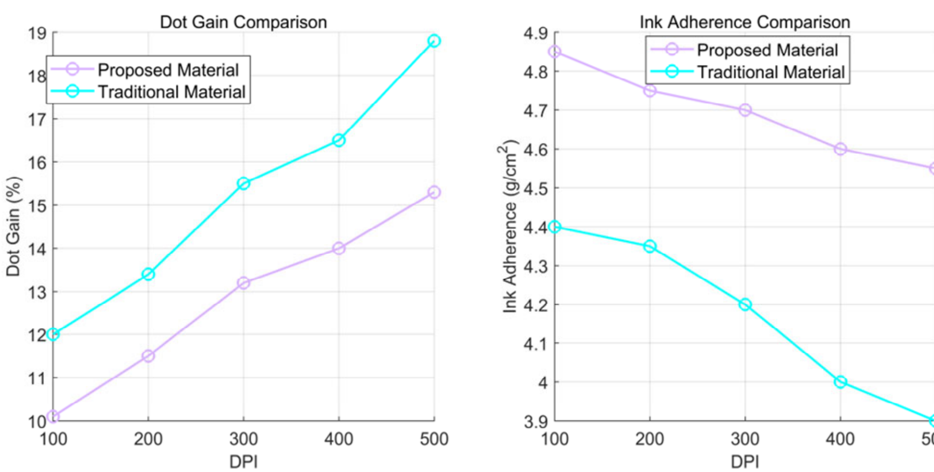

In Figure 7, the horizontal axis represents dots per inch (DPI), ranging from 100 to 500. The vertical axis shows the dot gain and ink adhesion of the two materials. For dot gain, the new material consistently shows lower values than the traditional material, indicating that it can better control print quality at high resolutions. As DPI increases, the dot gain rate of the new material gradually increases from 10.1% to 15.3%. In comparison, the traditional material shows a larger increase, from 12% to 18.8%, indicating that the printing effect of the new material at different resolutions is more stable and refined. In terms of ink adhesion, the adhesion of the new material is always higher than that of the traditional material. As the DPI increases, ink adhesion decreases slightly from 4.85 g/cm^2 to 4.55 g/cm^2, while the traditional material's adhesion decreases from

4.4 g/cm^2 to 3.9 g/cm^2. Overall, the new material outperformed traditional materials during printing, with more stable print quality, particularly at high resolutions. The new material also exhibited lower dot gain, indicating greater resistance to diffusion and better control over ink distribution on the paper surface. In terms of ink adhesion, the new material's higher adhesion indicates it bonds more effectively with the paper surface during printing, reducing ink peeling and improving printing quality.

5 Conclusions

This study successfully breaks through the technical bottleneck of large-scale application of intelligent responsive printing materials through innovations in material design, process optimisation, and system integration. At the material design level, the introduction of a dual-chamber microcapsule structure with temperature- and light-dependent responses has achieved the synergistic effect of multidimensional dynamic responses. The application of nano-interface crosslinkers significantly enhances the material's structural stability in hot, humid environments, resolving conflicts between environmental tolerance and material performance. In terms of process optimisation, precise control of the rheological properties of UV inks enables adaptation to the needs of high-speed screen/ink-jet printing, providing key technical support for large-scale production. In terms of system integration, the portable detection terminal based on smartphone spectral sensing and a dynamic recognition algorithm effectively bridges the gap between anti-counterfeiting characteristics and detection technology. The UV ink used in this scheme is a water-based system, which does not contain volatile organic solvents. The microcapsule synthesis uses emulsion polymerisation at room temperature, which offers low energy consumption, high yield, strong green manufacturing potential, and a large-scale cost advantage.

Declarations

The authors declare no conflict of interest

References

Alidaei-Sharif, H., Babazadeh-Mamaqani, M., Mohammadi-Jorjafki, M. et al. (2024) 'Multi-responsive polymer nanoparticles: a versatile platform for double-security anti-counterfeiting and smart food packaging', *Macromolecular Rapid Communications*, Vol. 45, No. 23, p.2400561.

Arslan, A., Roose, P., Houben, A. et al. (2023) 'Printability evaluation of UV-curable aqueous laponite/urethane-based PEG inks', *ACS Applied Polymer Materials*, Vol. 5, No. 4, pp.2345–2358.

Chen, H., Hu, H., Sun, B. et al. (2022) 'Dynamic anti-counterfeiting labels with enhanced multi-level information encryption', *ACS Applied Materials & Interfaces*, Vol. 15, No. 1, pp.2104–2111.

Chen, K., Chen, J., Xu, C. et al. (2025) 'Design and synthesis of multi-compartment microcapsules via pickering emulsion polymerization for infrared stealth and adaptive camouflage applications', *Small*, Vol. 21, No. 5, p.2405543.

Han, Y., Bao, S., Shi, B. et al. (2024) 'Fast and accurate recognition of perovskite fluorescent anti-counterfeiting labels based on lightweight convolutional neural networks', *ACS Applied Materials & Interfaces*, Vol. 16, No. 31, pp.41107–41118.

Huo, Y., Yang, Z., Wilson, T. et al. (2022) 'Recent progress in SERS-based anti-counterfeit labels', *Advanced Materials Interfaces*, Vol. 9, No. 17, p.2200201.

Iftekar, S.F., Aabid, A., Amir, A. et al. (2023) 'Advancements and limitations in 3D printing materials and technologies: a critical review', *Polymers*, Vol. 15, No. 11, p.2519.

Jafarzadeh, S., Nooshkam, M., Zargar, M. et al. (2024) 'Green synthesis of nanomaterials for innovative biopolymer packaging: challenges and outlooks', *Journal of Nanostructure in Chemistry*, Vol. 14, No. 2, pp.113–136.

Jongprasitkul, H., Turunen, S., Kellomäki, M. et al. (2024) 'A comprehensive study on rheological properties of photocrosslinkable gallol-metal complexed hyaluronic acid-based biomaterial inks', *Materials Advances*, Vol. 5, No. 14, pp.5823–5837.

Kim, H., Kim, J., Ryu, K.H. et al. (2023) 'Embedded direct ink writing 3D printing of UV curable resin/sepiolite composites with nano orientation', *ACS omega*, Vol. 8, No. 26, pp.23554–23565.

Lin, Y., Jiao, C., Qi, Y. et al. (2024) 'Multiple stimuli-responsive color-changing polymer materials for reversible writing and anti-counterfeiting', *ACS Applied Materials & Interfaces*, Vol. 16, No. 32, pp.43064–43071.

Lopez-Donaire, M.L., de Aranda-Izuzquiza, G., Garzon-Hernandez, S. et al. (2023) 'Computationally guided DIW technology to enable robust printing of inks with evolving rheological properties', *Advanced Materials Technologies*, Vol. 8, No. 3, p.2201707.

Ma, Y., Yu, Y., Li, J. et al. (2021) 'Stimuli-responsive photofunctional materials for green and security printing', *InfoMat*, Vol. 3, No. 1, pp.82–100.

Muthamma, K. and Sunil, D. (2022) 'Cellulose as an eco-friendly and sustainable material for optical anti-counterfeiting applications: an up-to-date appraisal', *ACS Omega*, Vol. 7, No. 47, pp.42681–42699.

Prosvirnina, A.P., Bugrov, A.N., Dobrodumov, A.V. et al. (2022) 'Bacterial cellulose nanofibers modification with 3-(trimethoxysilyl) propyl methacrylate as a crosslinking and reinforcing agent for 3D printable UV-curable inks', *Journal of Materials Science*, Vol. 57, No. 44, pp.20543–20557.

Shen, Y., Le, X., Wu, Y. et al. (2024) 'Stimulus-responsive polymer materials for multi-mode, multi-level information anti-counterfeiting: recent advances and future challenges', *Chemical Society Reviews*, Vol. 53, No. 2, pp.606–623.

Singh, S., Bhardwaj, S., Choudhary, N. et al. (2024) 'Stimuli-responsive chiral cellulose nanocrystals-based self-assemblies for security measures to prevent counterfeiting: a review', *ACS Applied Materials & Interfaces*, Vol. 16, No. 32, pp.41743–41765.

Soleimani-Gorgani, A., Najafi, F., Mohammadrezaei, F. et al. (2021) 'Transparent water-based UV-curable urethane acrylate ink-jet ink', *International Journal of Polymer Analysis and Characterization*, Vol. 26, No. 3, pp.228–239.

Su, H., Huang, C., Li, C. et al. (2023) 'Failure mechanism of the corrugated medium under simulated cold chain logistics', *ACS Omega*, Vol. 8, No. 26, pp.23673–23682.

Su, M. and Song, Y. (2021) 'Printable innovative materials and devices: strategies and applications', *Chemical Reviews*, Vol. 122, No. 5, pp.5144–5164.

Sun, H., Hwang, U., Kim, S. et al. (2025) 'Reversible thixotropic rheological properties of graphene-incorporated epoxy inks for self-standing 3D printing', *ACS Macro Letters*, Vol. 14, No. 2, pp.135–141.

Sun, Y., Le, X., Zhou, S. et al. (2022) 'Recent progress in smart polymeric gel-based information storage for anti-counterfeiting', *Advanced Materials*, Vol. 34, No. 41, p.2201262.

Wang, Q., Zhou, D., Gong, K. et al. (2024) 'A multidimensional anti-counterfeiting dynamic flexible label based on light/thermal responsive CLC microspheres', *Journal of Materials Chemistry C*, Vol. 12, No. 37, pp.15092–15100.

Wang, T., Zheng, H., Guo, Z. et al. (2024) 'Anti-counterfeiting textured pattern', *The Visual Computer*, Vol. 40, No. 3, pp.2139–2160.

Wu, K., Chen, Y., Zhang, Q. et al. (2024) 'Preparation of graphene oxide/polymer hybrid microcapsules via photopolymerization for double self-healing anticorrosion coatings', *ACS Applied Materials & Interfaces*, Vol. 16, No. 29, pp.38564–38575.

Yang, F., Wu, W., Deng, C. et al. (2025) 'Sustainable lignocellulosic room temperature phosphorescent inks for intelligent packaging and anti-counterfeiting', *ACS Sustainable Chemistry & Engineering*, Vol. 13, No. 19, pp.7199–7211.

Yin, Y. and Rogers, J.A. (2022) 'Introduction: innovative materials', *Chemical Reviews*, Vol. 122, No. 5, pp.4885–4886.

Zhang, C., Li, Y., Kang, W. et al. (2021) 'Current advances and future perspectives of additive manufacturing for functional polymeric materials and devices', *SusMat*, Vol. 1, No. 1, pp.127–147.

Zhou, D. and Miao, M. (2024) 'Research on cloud anti-counterfeiting product packaging design based on internet of things', *International Journal of Internet Manufacturing and Services*, Vol. 10, No. 1, pp.60–76.

Zhu, W., Tang, Y., Hu, S. et al. (2025) 'Three-dimensional printable triple-bonded polymer nanoparticles for invisible information encryption and robust anti-counterfeiting', *ACS Materials Letters*, Vol. 7, No. 6, pp.2343–2351.